
Coarse-to-Fine Q-attention: Efficient Learning for Visual Robotic Manipulation via Discretisation

Stephen James, Kentaro Wada, Tristan Laidlow, Andrew J. Davison

Dyson Robotics Lab

Imperial College London

{slj12, k.wada18, t.laidlow15, a.davison}@imperial.ac.uk

Abstract

Reflecting on the last few years, the biggest breakthroughs in deep reinforcement learning (RL) have been in the discrete action domain. Robotic manipulation, however, is inherently a continuous control environment, but these continuous control reinforcement learning algorithms often depend on actor-critic methods that are sample-inefficient and inherently difficult to train, due to the joint optimisation of the actor and critic. To that end, we explore how we can bring the stability of discrete action RL algorithms to the robot manipulation domain. We extend the recently released ARM algorithm, by replacing the continuous next-best pose agent with a discrete next-best pose agent. Discretisation of rotation is trivial given its bounded nature, while translation is inherently unbounded, making discretisation difficult. We formulate the translation prediction as the voxel prediction problem by discretising the 3D space; however, voxelisation of a large workspace is memory intensive and would not work with a high density of voxels, crucial to obtaining the resolution needed for robotic manipulation. We therefore propose to apply this voxel prediction in a coarse-to-fine manner by gradually increasing the resolution. In each step, we extract the highest valued voxel as the predicted location, which is then used as the centre of the higher-resolution voxelisation in the next step. This coarse-to-fine prediction is applied over several steps, giving a near-lossless prediction of the translation. We show that our new coarse-to-fine algorithm is able to accomplish RLBench tasks much more efficiently than the continuous control equivalent, and even train some real-world tasks, tabular rasa, in less than 7 minutes, with only 3 demonstrations. Moreover, we show that by moving to a voxel representation, we are able to easily incorporate observations from multiple cameras. Videos and code found at: <https://sites.google.com/view/c2f-q-attention>.

1 Introduction

In this paper, we are interested in a general real-world manipulation algorithm that can use a small number of demonstrations, along with a small amount of sparsely-rewarded exploration data, to accomplish a diverse set of tasks, both in simulation and the real world. To develop such an approach, two paradigms come to mind: imitation learning (IL) and reinforcement learning (RL). Imitation learning methods, such as behaviour cloning, suffer from compounding error due to covariate shift, while reinforcement learning suffers from long training times that often require millions of environment interactions. Recently however, Q-attention and the ARM system [1] has been shown to bypass many flaws that come with reinforcement learning, most notably the large training burden and difficulty with sparsely-rewarded and long-horizon tasks.

Unfortunately, like many modern continuous control RL algorithms, ARM’s next-best pose agent follows an actor-critic paradigm, which can be particularly unstable when learning from sparsely-rewarded and image-based tasks: two properties that are particularly important for robot manipulation tasks. In this paper, we re-examine how best to represent the continuous control actions needed for robot manipulation, abandoning the standard actor-critic approach, in favour of a simpler and more stable discrete action approach. The challenge therefore becomes how to effectively discretise 6D poses. Discretisation of rotation and gripper action is trivial given its bounded nature, but translation remains challenging given it is inherently unbounded. We solve this problem via a coarse-to-fine Q-attention, where we start with a coarse voxelisation of the translation space, use 3D Q-attention to identify the next most interesting point, and gradually make the resolution higher at each point.



Figure 1: C2F-ARM learns sparsely-rewarded tasks with only 3 demonstrations. Real-world tasks include: turning on a light, pulling cloth from shelf, pulling a toy car, taking a lid off a saucepan, and folding a towel.

With this new coarse-to-fine Q-attention, we present our Coarse-to-Fine Attention-driven Robotic Manipulation (C2F-ARM) system. We benchmark the system in simulation against other robot learning algorithms from both the reinforcement learning and imitation learning literature, and show that C2F-ARM is more sample-efficient and stable to train than other methods. We also show that C2F-ARM is capable of learning 5 diverse sets of sparsely-rewarded real-world tasks from only 3 demonstrations.

To summarise, the paper presents the following three contributions: **(1)** A novel way to discretise the unbounded translation space via coarse-to-fine Q-attention, allowing us to discard the often unstable actor-critic framework for a simpler deep Q-learning approach. **(2)** Our manipulation system, C2F-ARM, which uses the coarse-to-fine Q-attention along with a control agent to achieve sample-efficient learning of sparsely-rewarded tasks in both simulation and real-world. **(3)** The first use of a voxel representation for deep reinforcement learning for robot manipulation.

2 Related Work

Learning for manipulation

Recent trends in learning for manipulation have seen continuous-control reinforcement learning algorithms, such as TRPO [2], PPO [3], DDPG [4], TD3 [5], and SAC [6], trained on a variety of tasks, including cloth manipulation [7], lego stacking [8], pushing [9], and in-hand manipulation [10], to name but a few. These approaches rely on the actor-critic formulation, which is often sample-inefficient and unstable to train. Alternatively, discretisation, allows for simpler approaches, such as Q-learning. Our work is not the first use of discrete actions for visual manipulation; James *et al.* [11] discretised the joint space, where in each step the agent could choose to move one of the 6 joints by 1 degree; however, this method was sample-inefficient and inaccurate. An alternative to discretising the joint space, is to discretise the planar workspace, where pixels from a top-down camera act as high-level actions, such as pushing [12] or pick and place [13]. However, it is unclear how these can extend beyond top-down pick-and-place tasks, such as opening a microwave, opening an oven, and lifting a toilet seat. Our paper presents a full 6D manipulation system that can extend to a range of tasks, not just top-down ones.

Voxel representation for manipulation

Modelling 3D environments via voxels dates back as far as the 1980s [14, 15]. Since a voxel grid can store arbitrary values in each voxel, prior work has used it for various representations (geometry, semantics, learned features) for navigation and manipulation. Most works that use voxel

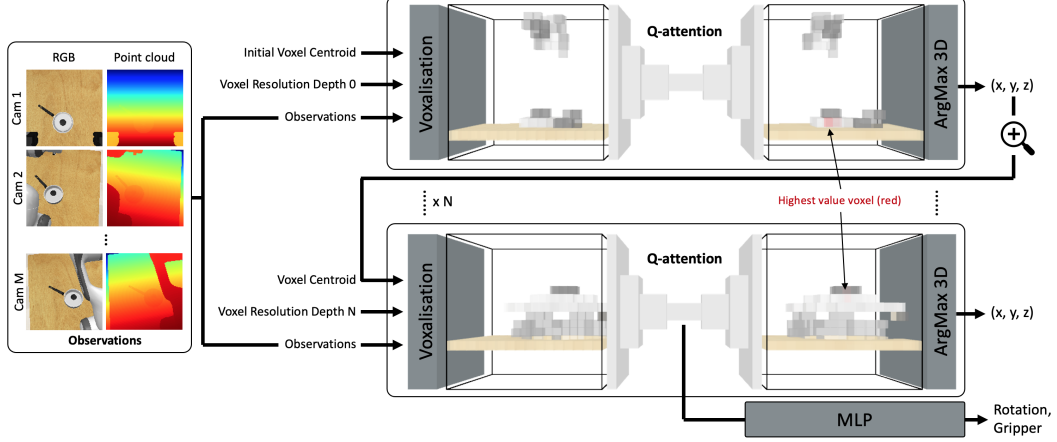


Figure 2: Summary of coarse-to-fine Q-attention. Observation data (RGB and point cloud) from M cameras are given to each depth of the Q-attention. At each level, the observations are voxelised at a given resolution and centred around a given point. The Q-attention gives the locations of the most interesting point in space, which is then used as the voxel centroid for the Q-attention at the next depth. Intuitively, this can be thought of as ‘zooming’ into a specific part of the scene to gain more accurate 3D information. The highlighted red voxel corresponds to the highest value.

representations use them for navigation [16, 17, 18]; however, some also use them for manipulation. Wada *et al.* [19] used a voxel grid to store occupancy and semantics of objects in a cluttered scene to select the next target object and grasp point. MoreFusion [20] is a system that uses voxels to perform multi-object reasoning to improve 6D pose estimation; the system gives accurate object poses and can perform precise pick-and-place in cluttered scenes. Recently, it has become common to use a voxel representation with a learning-based model. Song *et al.* [21] and Breyer *et al.* [22] fed a voxel grid representation to a neural network to generate 6DoF grasp actions. Prabhudesai *et al.* [23] built a learned 3D feature grid to generate actions from an unconstrained language. Although these learning-based voxel representation have been trained via large-scale supervised learning (i.e. demonstrations), in our work, we show that this representation is also useful in a reinforcement learning setting with only a few demonstrations.

3 Background

ARM [1] introduced several core concepts that facilitate the learning of robot manipulation tasks. These included Q-attention, keypoint detection, demo augmentation, and a high-level next-best pose action space. Most notable of these is the Q-attention, which is used in this work to discretise the unbounded translation space. We briefly outline Q-attention below.

Given an observation, \mathbf{o} (consisting of an RGB image, \mathbf{b} , an organised point cloud, \mathbf{p} , and proprioceptive data, \mathbf{z}), the Q-attention module, Q_θ , outputs 2D pixel locations of the next area of interest. This is done by extracting the coordinates of pixels with the highest value: $(x, y) = \arg \max_{\mathbf{a}'} 2D_{\mathbf{a}'} Q_\theta(\mathbf{o}, \mathbf{a}')$. These pixel locations are used to crop the RGB image and organised point cloud inputs and thus drastically reduce the input size to the next stage of the pipeline; this next stage is an actor-critic next-best pose agent. The parameters of the Q-attention are optimised by using stochastic gradient descent to minimise the loss:

$$J_Q(\theta) = \mathbb{E}_{(\mathbf{o}_t, \mathbf{a}_t, \mathbf{o}_{t+1}) \sim \mathcal{D}} [(\mathbf{r} + \gamma \max_{\mathbf{a}'} 2D_{\mathbf{a}'} Q_{\theta'}(\mathbf{o}_{t+1}, \mathbf{a}') - Q_\theta(\mathbf{o}_t, \mathbf{a}_t))^2 + \|Q\|], \quad (1)$$

where $Q_{\theta'}$ is the target Q-function, and $\|Q\|$ is the Q regularisation — an $L2$ loss on the per-pixel output of the Q function.

Algorithm 1 Coarse-to-Fine Attention-driven Robot Manipulation (C2F-ARM)

Initialise the N Q-attention networks $Q_{\theta_1}, \dots, Q_{\theta_N}$ with random parameters $\theta_1, \dots, \theta_N$.
Initialise target networks $\theta'_1 \leftarrow \theta_1, \dots, \theta'_N \leftarrow \theta_N$.
Initialise replay buffer \mathcal{D} with demos and apply keyframe selection and demo augmentation
for each iteration **do**
 for each environment step t **do**
 $\mathbf{o}_t \leftarrow (\mathbf{b}_t, \mathbf{p}_t, \mathbf{z}_t)$
 $\mathbf{c}^0 \leftarrow$ Scene centroid
 $\text{coords} \leftarrow []$ ▷ List to keep coords of each Q-attention depth
 for each (n of N) Q-attention depths **do**
 $\mathbf{v}^n \leftarrow \mathbf{V}(\mathbf{o}_t, \mathbf{e}^n, \mathbf{c}^n)$ ▷ Voxelise with given resolution & centroid
 $(x^n, y^n, z^n) \leftarrow \arg \max_{\mathbf{a}'} 3D_{\mathbf{a}'} Q_{\theta_n}(\mathbf{v}^n, \mathbf{a}')$ ▷ Use Q-attention to get voxel coords
 $\text{coords.append}((x^n, y^n, z^n))$
 if $n == N$ **then**
 $\alpha, \beta, \gamma, \omega \leftarrow \arg \max_{\mathbf{a}'} Q_{\theta_n}^h(\mathbf{v}^n, \mathbf{a}')$ for $h \in \{0, 1, 2, 3\}$ ▷ Rotation & gripper
 $\mathbf{c}^{n+1} \leftarrow (x^n, y^n, z^n)$ ▷ Voxel coords give centroid of next Q-attention depth
 $\mathbf{a}_t \leftarrow (\mathbf{c}^N, \alpha, \beta, \gamma, \omega)$ ▷ The next-best pose
 $\mathbf{o}_{t+1}, \mathbf{r} \leftarrow \text{env.step}(g)$
 $\mathcal{D} \leftarrow \mathcal{D} \cup \{(\mathbf{o}_t, \mathbf{a}_t, \mathbf{r}, \mathbf{o}_{t+1}, \text{coords})\}$ ▷ Store the transition in the replay buffer
 for each gradient step **do**
 $\theta_n \leftarrow \theta_n - \lambda_Q \hat{\nabla}_{\theta_n} J_Q(\theta_n)$ for $n \in \{0, \dots, N\}$ ▷ Update parameters
 $\theta'_n \leftarrow \tau \theta_n + (1 - \tau) \theta'_n$ for $n \in \{0, \dots, N\}$ ▷ Update target network weights

4 Method

Our system, C2F-ARM, can be split into 2 core phases. Phase 1 (Section 4.1) consists of the coarse-to-fine 3D Q-attention agent, which starts by voxelising the entire scene in a coarse manner, and then recursively makes the resolution finer until we are able to extract a continuous 6D next-best pose. Phase 2 (Section 4.2) is a low-level control agent that accepts the predicted next-best pose and executes a series of actions to reach the given goal pose. Before training, we fill the replay buffer with demonstrations using keyframe discovery and demo augmentation [1].

4.1 Coarse-to-fine Q-attention

The key contribution of this paper is the discretisation of the translation state space via the Q-attention, thereby allowing the use of discrete-action reinforcement learning algorithms to be used for recovering continuous actions. Our method formulates the translation prediction as a recursive, coarse-to-fine deep Q-network which accepts voxelised point cloud features, and outputs per-voxel Q-values. The highest-valued voxel represents the next-best voxel, whose location is used as the centre of a higher-resolution voxelisation in the next step. Note that ‘higher-resolution’ could be interpreted in one of 3 ways: (1) keeping the volume the same but increasing the number of voxels, (2) keeping the number of voxels the same but reducing the volume, or (3) a combination of both. We opt for (2), as this gives us the higher resolution, while keeping the memory footprint low. Intuitively, this coarse-to-fine Q-attention can be thought of as ‘zooming’ into a specific part of the scene to gain more accurate 3D information. The coarse-to-fine prediction is applied several times, which gives near-lossless prediction of the continuous translation. Rotation and gripper action prediction is simpler due to its bounded nature; these are predicted in the final depth of the Q-attention as an additional branch. The coarse-to-fine Q-attention is summarised in Figure 2.

Formally, we define a voxelisation function $\mathbf{v}^n = \mathbf{V}(\mathbf{o}, \mathbf{e}^n, \mathbf{c}^n)$, which takes the observation \mathbf{o} , a voxel resolution \mathbf{e}^n , and a voxel grid centre \mathbf{c}^n , and returns a voxel grid $\mathbf{v}^n \in \mathbb{R}^{xyz(3+M+1)}$ at depth n , where n is the depth/iteration of the Q-attention, and where each voxel contains the 3D coordinates, M features (e.g. RGB values, features, etc), and an occupancy flag.

Given our Q-attention function Q_{θ_n} at depth n , we extract the indicies of the voxel with the highest value:

$$\mathbf{v}_{ijk}^n = \arg \max_{\mathbf{a}'} 3D_{Q_{\theta_n}}(\mathbf{o}, \mathbf{a}'), \quad (2)$$

where \mathbf{v}_{ijk} is the extracted voxel index located at (i, j, k) .

By offsetting the centre of the current voxelisation with the extracted indicies, we can trivially extract the (x^n, y^n, z^n) location of that voxel. For ease of readability, we henceforth assume that $\arg \max 3D$ also performs the conversion to world coordinates, to directly give (x^n, y^n, z^n) . As the extracted coordinates represent the next-best coordinate to voxelise at a higher resolution, we set these coordinates to be the voxel grid centre \mathbf{c} for the next depth: $\mathbf{c}^{n+1} = (x^n, y^n, z^n)$. However, if this is the last depth of the Q-attention, then \mathbf{c}^{n+1} represents the continuous representation of the translation (i.e. the translation component of the next-best pose agent). The rotation component of the pose (and gripper action) are recovered from an MLP branch of the final Q-attention depth:

$$\alpha, \beta, \gamma, \omega \leftarrow \arg \max_{\mathbf{a}'} Q_{\theta_N}^h(\mathbf{v}^n, \mathbf{a}') \text{ for } h \in \{0, 1, 2, 3\}, \quad (3)$$

where α, β, γ represent the individual rotation axis, and ω is the gripper action.

Each depth of the Q-attention can be thought as its own reinforcement learning task, where the voxelised portion of the scene is treated as the ‘environment’, and voxel indices are treated as the ‘actions’. The coarse-to-fine Q-attention shares the same motivation that was laid out in ARM [1], i.e. that our gaze focuses sequentially on objects being manipulated [24], however, its role in the manipulation system is different. ARM [1] uses Q-attention to reduce the image resolution to a next-best pose phase (by cropping 128×128 observations to 16×16), while the role of coarse-to-fine Q-attention is to discretise the otherwise unbounded translation space. This highlights the versatility of Q-attention.

4.2 Control Agent

The control agent remains largely unchanged from ARM [1]. Given the next-best pose suggestion from the previous stage, we give this to a goal-conditioned control function $f(\mathbf{s}_t, \mathbf{g}_t)$, which given state \mathbf{s}_t and goal \mathbf{g}_t , outputs motor velocities that drives the end-effector towards the goal. This function can take on many forms, but two noteworthy solutions would be either motion planning in combination with a feedback-control or a learnable policy trained with imitation/reinforcement learning. Given that the environmental dynamics are limited in the benchmark, we opted for the motion planning solution.

Given the target pose, we perform path planning using the SBL [25] planner within OMPL [26], and use Reflexxes Motion Library for on-line trajectory generation. If the target pose is out of reach, we terminate the episode and supply a reward of -1 . The only difference from ARM [1] in this stage, is that the path planning does perform collision checking during planning; our action mode is conveniently encapsulated by the ‘*ABS_EE_POSE_PLAN_WORLD_FRAME_WITH_COLLISION_CHECK*’ action mode in RL Bench [27].

5 Results

The results can be broken into three core sections: (1) simulation results using RL Bench [27] to benchmark our algorithm against other popular robot learning algorithms using only the front-facing camera. (2) additional simulation results in RL Bench where we evaluate our method on additional tasks and perform an ablation study into the robustness of the coarse-to-fine approach. (3) Real-world results where we show that the sample-efficiency in simulation is also present when training from scratch in the real world.

5.1 Simulation

For our simulation experiments, we use RL Bench [27]. RL Bench was chosen due to its emphasis on vision-based manipulation benchmarking and because it gives access to a wide variety of tasks with demonstrations. Each task has a completely sparse reward of 100 which is given only on task completion, and 0 otherwise.

Comparison to other Robot Learning Methods

To compare to other robot learning methods, we select the same 8 tasks as in James *et al.* [1]; these are task that are achievable from using only the front-facing camera. Figure 3 shows the results of

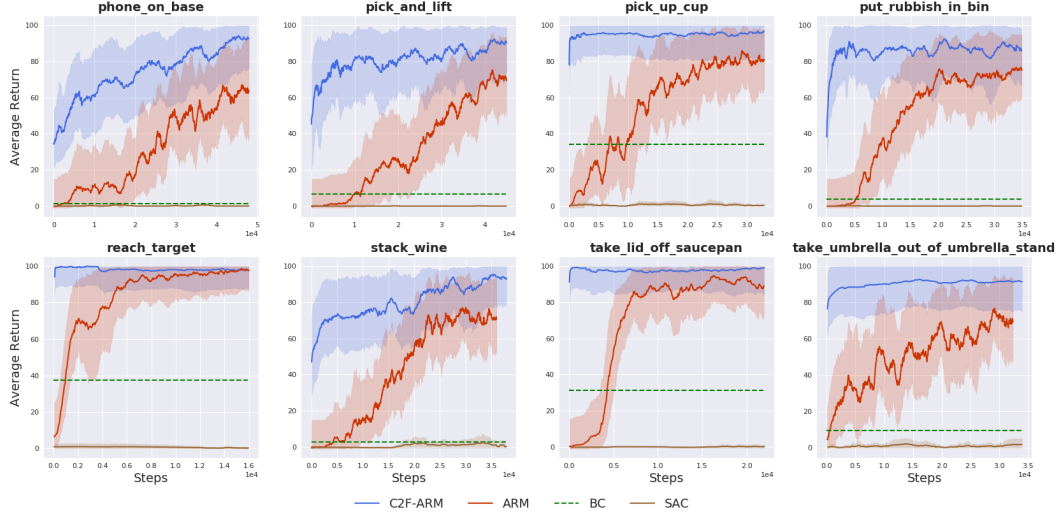


Figure 3: Learning curves for 8 RL Bench tasks. In addition to our method (C2F-ARM), we include the same baselines as in previous work: ARM [1], SAC [6], and behaviour cloning (BC). Note that our method **only receive 10 demos**, while all other baselines receiving 100 demos which are stored in the replay buffer prior to training. Solid lines represent the average evaluation over 5 seeds, where the shaded regions represent the *min* and *max* values across those trials.

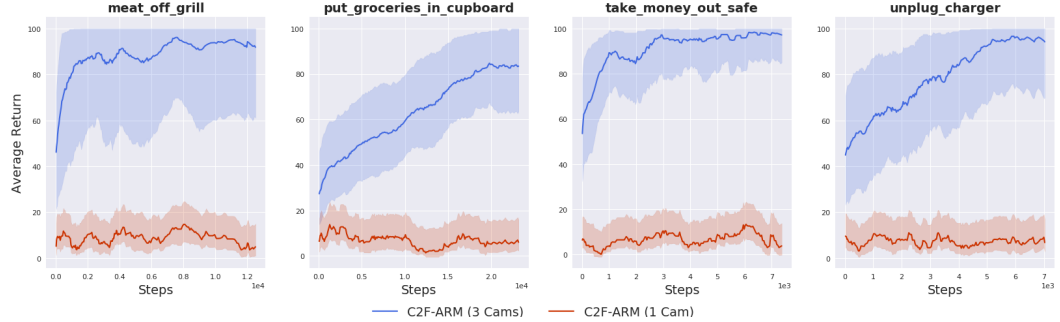


Figure 4: Learning curves for 4 additional RL Bench tasks that are difficult or impossible to achieve with only the front-facing camera. The 3 cameras used are the wrist, left shoulder, and right shoulder. Solid lines represent the average evaluation over 5 seeds, where the shaded regions represent the *min* and *max* values across those trials.

this comparison. Our baselines include ARM [1], SAC [6], and behavioural cloning (BC). Other baselines were attempted, such as DAC [28] (an improved, off-policy version of GAIL [29]) and TD3 [5], but these were unsuccessful. As noted in James *et al.* [1], we were unable to find work that has successfully trained DAC [28] from images, and TD3 was omitted due to being less successful than SAC (as has been shown in prior work [6]). The results in Figure 3 show that our method outperforms ARM[1] by a large margin; either by attaining an overall higher performance, or attaining the same performance but in substantially less environment steps. We also note as a purely qualitative observation, that C2F-ARM required little to no hyperparameter tuning, while baselines required a substantial amount. Code has been included on the project website which includes C2F-ARM, ARM, SAC, BC, DAC, and TD3.

All method (C2F-ARM, ARM, SAC, and BC) feature keyframe discovery and demo augmentation [1], and receive the same demonstration sequences, which are loaded into the replay buffer prior to training. Note that C2F-ARM does not require as many demonstrations as the other methods (as is evident in Section 5.2), and so is given only 10 demos, while baselines receive 100. Each Q-attention layer follows a light-weight U-Net style architecture [30], but uses 3D convolutions rather than 2D ones. Our U-Net encoder features 3 Inception-style blocks [31], with 64 input-output channels, and a

3×3 maxpool after each block, while our U-Net decode features 3 Inception-Upsample-Inception blocks. Note that the final Q-attention layer is also used for the rotation and gripper prediction; this is achieved by concatenating the maxpooled and soft-argmax values after each of the Inception blocks in the decoder, and sending them through 2 fully connected layers each with 256 nodes. Finally, these features are passed through a final fully-connected layer which gives the rotation and gripper discretisation. The voxel resolution at each depth was set to 0.01, while the initial voxel centroid was set to be the centre of the scene. Voxelisation code has been adapted from Ivy [32]. Baselines use the same architectures as presented in James *et al.* [1].

Multi-camera and Ablations

The second set of simulation experiments evaluates C2F-ARM in with multiple cameras. One of the weaknesses of ARM [1] was its inability to trivially handle multi-camera environments; for this reason, tasks were chosen that could be done with only the front-facing camera. However, many tasks in RL Bench (and the real world) often require more than one camera. For this reason, Figure 4 shows an additional 4 tasks from RL Bench which we believe to be difficult to accomplish by only using the front-facing camera. For each of these tasks, we run our method using 3 cameras (wrist, left shoulder, and right shoulder), and compare this to using only the front-facing camera. Due to the voxelised nature of C2F-ARM, no part of the system needs to be modified when using additional cameras. The results in Figure 4 clearly show that these tasks cannot be done with only a single camera, and that C2F-ARM can perform well when given the appropriate camera information.

For the final set of simulation experiments, we evaluate how robust C2F-ARM is when altering the number of Q-attention layers and the volume of the voxels. Figure 5 shows that all resolutions and number of layers eventually learn the tasks, but to varying degrees. Note that the coarsest setup (8, 8) understandably performs the worst, as there are only two layers of a very coarse 8^3 voxel grid, making the scene understanding phase difficult. We hypothesise that voxelising image features (rather than raw RGB values) would perform better at these coarser setups; we leave this for future work.

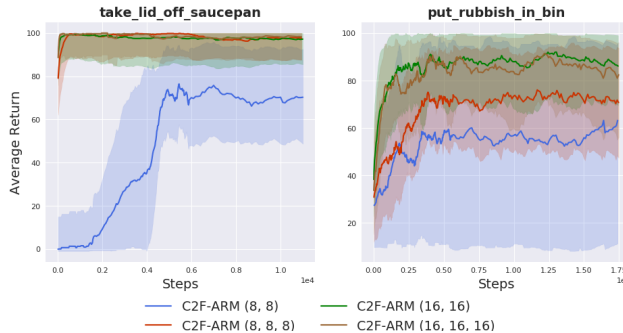


Figure 5: Investigation of the Q-attention depth and voxel volume across the easier ‘take_lid_off_saucepan’ task and harder ‘put_rubbish_in_bin’ task.

5.2 Real World

To further show the sample efficiency of our method, we train on 5 real-world tasks from scratch, which can be seen in Figure 6. At the beginning of each episode, the objects in the tasks are moved randomly within the robot workspace. We train each of the tasks until the agent achieves 4 consecutive successes. The approximate time to train each task are: pulling cloth from shelf (~ 26 minutes), pulling a toy car (~ 18 minutes), taking a lid off a saucepan (~ 6 minutes), folding a towel (~ 24 minutes), and turning on a light (~ 42 minutes). We use the Franka Emika Panda, and a single RGB-D RealSense camera. All tasks receive 3 demonstrations which are given through the HTC Vive VR system. These qualitative results are best seen via the full, uncut training video of each of the 5 tasks, located on the project website ¹.

6 Discussion and Conclusion

We have presented Coarse-to-Fine Attention-driven Robot Manipulation (C2F-ARM), which is an algorithm that utilises a coarse-to-fine Q-attention and allows discretisation of the translation space. With this discretisation, we are able to diverge from unstable actor-critic methods and instead use a more stable deep Q-learning method. As a result, we end up with a sample-efficient robot learning algorithm that outperforms others and can learn real-world tasks in an hour or less.

¹ <https://sites.google.com/view/c2f-q-attention>

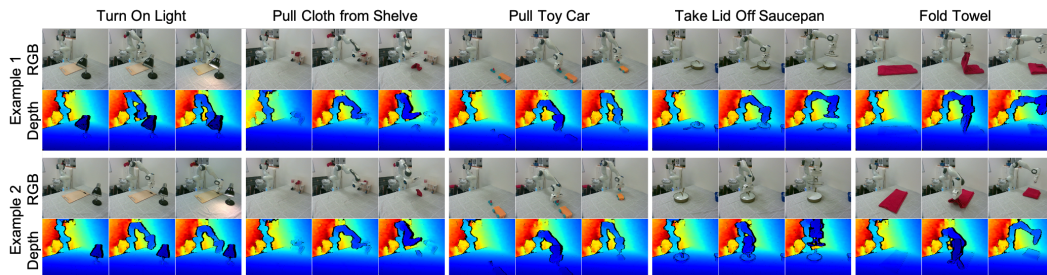


Figure 6: Two examples of successful trials performed with C2F-ARM on the tasks: turn on light, pull cloth from shelf, pull toy car, take lid off saucepan, and fold towel. The agent only received 3 demonstrations. Each column for each tasks shows the RGB-D observations at $t = 0$, $t = \frac{T}{2}$, and $t = T$.

C2F-ARM can be considered as an improved, discrete-action version of ARM [1]. There are 3 key differences to the original ARM system: (1) the role and architecture of Q-attention has changed; in ARM, the role of the 2D Q-attention was to act as a hard-attention that would give crops to the actor-critic next-best-pose agent, whereas in C2F-ARM the role of the 3D Q-attention is to be recursively applied in a coarse-to-fine manner in order to discretise the unbounded translation space. (2) The number of stages in the system has decreased; ARM was a 3-stage system, consisting of Q-attention, next-best-pose agent, and the control agent, whereas C2F-ARM removes the need for the actor-critic next-best-pose agent, and so consists only of the coarse-to-fine Q-attention and control agent. (3) C2F-ARM seamlessly supports multiple cameras or a single moving camera; ARM was not suited for multiple cameras, due to the undefined behaviour when a camera observation did not feature any interesting pixels, and was not suited for a moving camera due to the potential that the crop size may be too small or big to correctly crop when the camera was near or far to an interesting object. C2F-ARM does not suffer from this because all cameras are voxelised to a canonical world frame.

There are a number of areas for improvement. Currently, only raw RGB and point-cloud data are stored in the voxels, but we hypothesise that adding a small convolutional network to extract pixel features could allow for more expressive voxel values, especially when dealing with small resolutions or a small number of coarse-to-fine Q-attention layers. Another weakness is that we are restricted to keeping the initial voxel resolution (at Q-attention depth 0) to be reasonably small. This is not an issue when considering manipulation on a fixed table, but becomes an issue when considering mobile manipulation, where the resolution at depth 0 may have to become very large to accommodate voxelising an entire room or house; we look to investigating solutions to this in future work. Much like ARM [1], the control agent uses path planning and on-line trajectory generation, but will undoubtedly require improvement for achieving tasks that have dynamic environments (e.g. moving target objects, moving obstacles, etc) or complex contact dynamics (e.g. peg-in-hole). The work that we are most excited about is exploring the use of this system in multi-task [33] and few-shot [34, 35] learning scenarios.

Acknowledgements

Research presented in this paper has been supported by Dyson Technology Ltd.

References

- [1] Stephen James and Andrew J. Davison. Q-attention: Enabling efficient learning for vision-based robotic manipulation. *arXiv preprint arXiv:2105.14829*, 2021.
- [2] John Schulman, Sergey Levine, Pieter Abbeel, Michael Jordan, and Philipp Moritz. Trust region policy optimization. In *International conference on machine learning*, pages 1889–1897. PMLR, 2015.

- [3] John Schulman, Filip Wolski, Prafulla Dhariwal, Alec Radford, and Oleg Klimov. Proximal policy optimization algorithms. *arXiv preprint arXiv:1707.06347*, 2017.
- [4] Timothy P Lillicrap, Jonathan J Hunt, Alexander Pritzel, Nicolas Heess, Tom Erez, Yuval Tassa, David Silver, and Daan Wierstra. Continuous control with deep reinforcement learning. *Intl. Conference on Learning Representations*, 2015.
- [5] Scott Fujimoto, Herke Van Hoof, and David Meger. Addressing function approximation error in actor-critic methods. *Intl. Conference on Machine Learning*, 2018.
- [6] Tuomas Haarnoja, Aurick Zhou, Kristian Hartikainen, George Tucker, Sehoon Ha, Jie Tan, Vikash Kumar, Henry Zhu, Abhishek Gupta, Pieter Abbeel, et al. Soft actor-critic algorithms and applications. *arXiv preprint arXiv:1812.05905*, 2018.
- [7] Jan Matas, Stephen James, and Andrew J Davison. Sim-to-real reinforcement learning for deformable object manipulation. *Conference on Robot Learning*, 2018.
- [8] Tuomas Haarnoja, Vitchyr Pong, Aurick Zhou, Murtaza Dalal, Pieter Abbeel, and Sergey Levine. Composable deep reinforcement learning for robotic manipulation. In *2018 IEEE International Conference on Robotics and Automation (ICRA)*, pages 6244–6251. IEEE, 2018.
- [9] Lerrel Pinto, Marcin Andrychowicz, Peter Welinder, Wojciech Zaremba, and Pieter Abbeel. Asymmetric actor critic for image-based robot learning. *Robotics: Science and Systems*, 2018.
- [10] Aravind Rajeswaran, Vikash Kumar, Abhishek Gupta, Giulia Vezzani, John Schulman, Emanuel Todorov, and Sergey Levine. Learning complex dexterous manipulation with deep reinforcement learning and demonstrations. *Robotics: Science and Systems*, 2018.
- [11] Stephen James and Edward Johns. 3D simulation for robot arm control with deep Q-learning. *Conference on Neural Information Processing Systems Workshop (Deep Learning for Action and Interaction)*, 2016.
- [12] Andy Zeng, Shuran Song, Stefan Welker, Johnny Lee, Alberto Rodriguez, and Thomas Funkhouser. Learning synergies between pushing and grasping with self-supervised deep reinforcement learning. In *IEEE Intl. Conference on Intelligent Robots and Systems*, pages 4238–4245. IEEE, 2018.
- [13] Andy Zeng, Pete Florence, Jonathan Tompson, Stefan Welker, Jonathan Chien, Maria Attarian, Travis Armstrong, Ivan Krasin, Dan Duong, Vikas Sindhwani, et al. Transporter networks: Rearranging the visual world for robotic manipulation. *Conference on Robot Learning*, 2020.
- [14] Yuval Roth-Tabak and Ramesh Jain. Building an environment model using depth information. *Computer*, 22(6):85–90, 1989.
- [15] H Moravec. Robot spatial perception by stereoscopic vision and 3D evidence grids. *Perception*, 1996.
- [16] Armin Hornung, Kai M Wurm, and Maren Bennewitz. Humanoid robot localization in complex indoor environments. In *2010 IEEE/RSJ International Conference on Intelligent Robots and Systems*, pages 1690–1695. IEEE, 2010.
- [17] Ivan Dryanovski, William Morris, and Jizhong Xiao. Multi-volume occupancy grids: An efficient probabilistic 3D mapping model for micro aerial vehicles. In *2010 IEEE/RSJ International Conference on Intelligent Robots and Systems*, pages 1553–1559. IEEE, 2010.
- [18] Armin Hornung, Mike Phillips, E Gil Jones, Maren Bennewitz, Maxim Likhachev, and Sachin Chitta. Navigation in three-dimensional cluttered environments for mobile manipulation. In *2012 IEEE International Conference on Robotics and Automation*, pages 423–429. IEEE, 2012.
- [19] Kentaro Wada, Kei Okada, and Masayuki Inaba. Probabilistic 3D multilabel real-time mapping for multi-object manipulation. In *2017 IEEE/RSJ International Conference on Intelligent Robots and Systems (IROS)*, pages 5092–5099. IEEE, 2017.

- [20] Kentaro Wada, Edgar Sucar, Stephen James, Daniel Lenton, and Andrew J Davison. MoreFusion: Multi-object reasoning for 6D pose estimation from volumetric fusion. In *IEEE Conference on Computer Vision and Pattern Recognition*, pages 14540–14549, 2020.
- [21] Shuran Song, Andy Zeng, Johnny Lee, and Thomas Funkhouser. Grasping in the wild: Learning 6dof closed-loop grasping from low-cost demonstrations. *IEEE Robotics and Automation Letters*, 5(3):4978–4985, 2020.
- [22] Michel Breyer, Jen Jen Chung, Lionel Ott, Roland Siegwart, and Juan Nieto. Volumetric grasping network: real-time 6 dof grasp detection in clutter. *arXiv preprint arXiv:2101.01132*, 2021.
- [23] Mihir Prabhudesai, Hsiao-Yu Fish Tung, Syed Ashar Javed, Maximilian Sieb, Adam W Harley, and Katerina Fragkiadaki. Embodied language grounding with implicit 3D visual feature representations. *arXiv preprint arXiv:1910.01210*, 2019.
- [24] Michael Land, Neil Mennie, and Jennifer Rusted. The roles of vision and eye movements in the control of activities of daily living. *Perception*, 28(11):1311–1328, 1999.
- [25] Gildardo Sánchez and Jean-Claude Latombe. A single-query bi-directional probabilistic roadmap planner with lazy collision checking. In *Robotics research*, pages 403–417. Springer, 2003.
- [26] Ioan A. Şucan, Mark Moll, and Lydia E. Kavraki. The Open Motion Planning Library. *IEEE Robotics & Automation Magazine*, 19(4):72–82, December 2012. <https://ompl.kavrakilab.org>.
- [27] Stephen James, Zicong Ma, David Rovick Arrojo, and Andrew J. Davison. RL Bench: The robot learning benchmark & learning environment. *IEEE Robotics and Automation Letters*, 2020.
- [28] Ilya Kostrikov, Kumar Krishna Agrawal, Debidatta Dwibedi, Sergey Levine, and Jonathan Tompson. Discriminator-actor-critic: Addressing sample inefficiency and reward bias in adversarial imitation learning. *Intl. Conference on Learning Representations*, 2019.
- [29] Jonathan Ho and Stefano Ermon. Generative adversarial imitation learning. *Advances in Neural Information Processing Systems*, 2016.
- [30] Olaf Ronneberger, Philipp Fischer, and Thomas Brox. U-net: Convolutional networks for biomedical image segmentation. In *International Conference on Medical image computing and computer-assisted intervention*, pages 234–241. Springer, 2015.
- [31] Christian Szegedy, Wei Liu, Yangqing Jia, Pierre Sermanet, Scott Reed, Dragomir Anguelov, Dumitru Erhan, Vincent Vanhoucke, and Andrew Rabinovich. Going deeper with convolutions. In *Proceedings of the IEEE conference on computer vision and pattern recognition*, pages 1–9, 2015.
- [32] Daniel Lenton, Fabio Pardo, Fabian Falck, Stephen James, and Ronald Clark. Ivy: Templated deep learning for inter-framework portability. *arXiv preprint arXiv:2102.02886*, 2021.
- [33] Dmitry Kalashnikov, Jacob Varley, Yevgen Chebotar, Benjamin Swanson, Rico Jonschkowski, Chelsea Finn, Sergey Levine, and Karol Hausman. MT-Opt: Continuous multi-task robotic reinforcement learning at scale. *arXiv preprint arXiv:2104.08212*, 2021.
- [34] Stephen James, Michael Bloesch, and Andrew J Davison. Task-embedded control networks for few-shot imitation learning. In *Conference on Robot Learning*, pages 783–795. PMLR, 2018.
- [35] Alessandro Bonardi, Stephen James, and Andrew J Davison. Learning one-shot imitation from humans without humans. *IEEE Robotics and Automation Letters*, 5(2):3533–3539, 2020.